The successional formation and release of domoic acid in a *Pseudo-nitzschia* bloom in the Juan de Fuca Eddy: a drifter study.

C. G. Trick[1,2*], *V.L. Trainer*[3], *W. P. Cochlan*[4], *Mark L. Wells*[5], *and B.F. Beall*[1,6]

[1] Department of Biology, Western University, London, Ontario, N6A 5B7 Canada.

[2] Interfaculty Program in Public Health, Schulich School of Medicine and Dentistry, London, Ontario, N6G 2M1 Canada.

[3] Environmental and Fisheries Science Division, National Marine Fisheries Service, [4] Northwest Fisheries Science Center, National Oceanic and Atmospheric Administration, Seattle, WA 98112, USA.

[4] Estuary and Ocean Science Center, San Francisco State University, Tiburon, CA 94920-1205, USA.

[5] School of Marine Science, University of Maine, Orono, ME 04469, USA.

[6] Current Address: Environmental Resources Management, Vancouver, BC, V6E 2J3 Canada

***Corresponding Author**:* Department of Biology, Room 402, North Campus Building, 1151 Richmond St. N., Western University, London, Ontario, Canada N6B 3E5.
E-mail: trick@uwo.ca, Phone: (519) 661-3899

Abstract

Blooms of *Pseudo-nitzschia* species are frequent, but presently unpredictable, in the Juan de Fuca Eddy region off the coasts of Washington (US) and British Columbia (Canada). This upwelling eddy region is proposed to be the bloom initiation site, from nutrients upwelled to the surface, before cells are entrained into the coastal surface currents. During a shipboard study, we characterized the different stages of the *Pseudo-nitzschia* bloom development from its initiation and intensification, to its eventual sinking and dissipation. Specifically, we followed a water mass using lagrangian ARGOS-tracked drifters released at the eddy water mass and quantified production of dissolved and particulate domoic acid, and the physiological status of the *Pseudo-nitzschia* cells with regards to photosynthesis, nutrient needs and sinking rates, along with its relationship with competing species – in this case, the marine euglenoid, *Eutreptiella* spp. The drifter study allows for an interpretation of the presence or absence of *Pseudo-nitzschia* and domoic acid against active environmental factors – particularly copper and iron.

Key Words: algal biotoxins, amnesic shellfish poisoning, copper, DFB, domoic acid, Harmful Algal Blooms, iron, Juan de Fuca Eddy, *Pseudo-nitzschia*, Washington State

1. Introduction

The Juan de Fuca eddy is a nutrient-rich, physically retentive region off the northwestern U.S. coast that serves as an initiation site for toxigenic diatoms of the *Pseudo-nitzschia* genus Pergallo [Heterokonta, Bacillariophyceae] (Trainer et al., 2002; Trainer and Hickey, 2009; Hickey et al., 2013). This region serves as a natural laboratory for studying the *Pseudo-nitzschia* cells, and the oceanographic progression of the blooms at the eddy core, where nutrients are introduced, to the possible intersection of the bloom to the coastline (Adams et al., 2000, Trainer et al., 2002), where domoic acid is introduced to economically, socially, and culturally significant shellfish populations (Chadsey et al., 2011; Dyson and Huppert, 2010). Less studied are the physiological changes associated with the progression of *Pseudo-nitzschia* from the bloom initiation site to the presumably more mature bloom some distance and time away from the initiation site.

Historically, researchers have used a spatial census method to systematically acquire and record data about the members of a given bloom-forming population. This approach is valuable, links well with standardized surveys for physical and chemical profiles and provides a spatial template from which the trajectory and path of the bloom cells can be transcribed. The alternative is to plan the research and cruise track "to follow the bloom", or rather, to follow a drifter over time that is designed to track water at a specific depth – water that contains the planktonic bloom cells under study. This Lagrangian approach is comparable to a population cohort survey, where the same population is followed over time, and key population factors such as growth, loss, photosynthetic efficiency and physiological health can be assessed within the bloom

65 (Lewitus et al., 2012; Trainer et al., 2012a). This latter approach enables measurements
66 at one point in time to be confidently connected with previous and future measurements
67 The Ecology and Oceanography of Harmful Algal Blooms in the Pacific Northwest
68 (ECOHAB-PNW) was a 5-year, 6-cruise multi-disciplinary project that measured
69 physical, chemical, and biological parameters associated with the periodic blooms of
70 *Pseudo-nitzschia* species off the coasts of Washington State and Vancouver Island,
71 British Columbia including the entrance waters of the Strait of Juan de Fuca. In
72 September 2004, the cruise strategy included the release of Lagrangian ARGOS-tracked
73 drifters that when placed at the sources of nutrients (eddy core; Hickey et al., 2006;
74 MacPhadyen et al., 2008) enabled the longitudinal study of the phytoplankton
75 community. The multi-week cruise occurred during a large, nearly monospecific diatom
76 bloom of *P. cuspidata* that co-dominated the phytoplankton assemblage with the
77 euglenoid, *Eutreptiella* spp. (Trainer et al., 2009b). There were no significant
78 correlations between the observed domoic acid (DA) concentrations [particulate DA
79 (pDA) and cellular DA] and the ambient concentrations of macronutrients (nitrate,
80 orthophosphate and silicate) (Trainer et al. 2009b). As with the majority of the spatial
81 census cruises, neither were correlations detected between pDA or *Pseudo-nitzschia*
82 concentrations and total bacteria or cyanobacteria abundances. Combined with the
83 correlational assessment of environmental, ecological and toxicological data, we used a
84 series of grow-out experiments to consider if the postulate that domoic acid acted as a
85 ligand to bind either copper or iron (Rue and Bruland, 2001), improving the
86 physiological health of the cells as these putatively limiting trace metals were
87 scavenged from the environment (Maldonado et al., 2002; Wells et al., 2005), enabling
88 Pseudo-nitzschia to achieve less restricted physiological health Here we demonstrate

how the independent nature of *Pseudo-nitzschia* is best revealed by the variation in two trace metals – copper and iron – working in conjunction with particulate and dissolved DA levels.

2. Materials and methods

2.1. Cruise

The ECOHAB-PNW-III cruise was carried out aboard the R/V *Atlantis* (AT11-17) during 8-28 September 2004. The initial survey region for a large-scale synoptic assessment covered *ca.* 12,000 km^{-2}, spanning a N-S latitude line from 48.7°N to 47.0 °N, along a longitude of 125.0°W. The synoptic scale survey grid was designed to include areas influenced by the Strait of Juan de Fuca, the Juan de Fuca Eddy region and the coastal upwelling region off the Washington coast.

2.2. Drifters

Lagrangian ARGOS-tracked drifters (Brightwater Instrument Co. models 104a and 115) were deployed to delineate patterns and speeds of surface flows in the eddy area, as well as to determine the ultimate fate of eddy water. These drifter models were designed according to the Davis/CODE configuration to accurately track the upper 1 m of the water column (Davis, 1985), and transmitted ½ hourly GPS position to the ARGOS satellites. Drifter A was deployed in the outer eddy at 21:00 h on September 16 and was followed for 10 days.

2.3. Satellite imagery

Sea-viewing wide field-of-view sensor (SeaWiFS) imagery was acquired from the National Oceanic and Atmospheric Administration's (NOAA) Coastwatch Program. The images were processed with the latest version of SeaWiFS data analysis system (SeaDAS 4.0), which uses an atmospheric correction that compensates for near-infrared water leaving radiance and absorbing aerosols (Gordon and Wang, 1994; Stumpf et al., 2003). The resulting chlorophyll imagery was developed using the global OC4 algorithm, with 1 km resolution (O'Reilly et al., 2000).

2.4. Chlorophyll a

Surface samples were analyzed for phytoplankton biomass as chlorophyll a (chl-*a* L^{-1}) using the non-acidification *in vitro* fluorometric technique (Welschmeyer, 1994). Seawater was filtered onto glass fiber filters (Whatman GF/F filters; 25-mm diameter, 0.7 µm nominal pore size) at low pressure (<70 kPa) and immediately extracted in 90% acetone for approximately 24 h at -20°C. Chl-*a* concentrations were determined with a Turner Designs 10AU fluorometer calibrated at the beginning of each cruise with pure chl-*a* in 90% acetone and monitored for instrument drift during the cruise using a solid secondary standard.

2.5. Nutrients

Water samples for dissolved inorganic macronutrient analyses were collected at a depth of 5 m using a 10 L Niskin bottle. Unfiltered samples were collected in pre-cleaned polypropylene tubes and freshly analyzed at sea for nitrate plus nitrite (NO_3^- + NO_2^-; hereafter referred to as nitrate), orthophosphate (PO_4^{3-}), and silicate [$Si(OH)_4$] with a Lachat QuikChem8000 Flow Injection Analysis system using standard

136 calorimetric techniques (Smith and Bogren, 2001; Knepel and Bogren, 2002; Wolters,
137 2002; respectively).
138
139 *2.6. Domoic acid*
140 Dissolved DA (dDA) and particulate DA (pDA) concentrations were measured
141 on sample filtrates and filters, respectively (Millipore Corp. mixed cellulose ester filters;
142 0.45 µm) using the direct competitive enzyme linked immunoassay (cELISA) Biosense
143 kits (Biosense Laboratories, Bergen, Norway), a modified version of the indirect
144 cELISA method as described in Garthwaite et al. (1998). Samples were analyzed in
145 duplicate, and the occasional poor replicates reanalyzed. The limit of detection for
146 seawater samples was 6.8 ng L^{-1}, and the limit of quantification was 13.9 ng L^{-1}.
147 Cellular DA concentrations were estimated by dividing pDA concentrations by the
148 corresponding *Pseudo-nitzschia* cell concentrations. These estimates were restricted to
149 samples containing a minimum of 50 cells, providing a 95% confidence interval of ±
150 30% of the mean cell density (Lund et al. 1958). As the focus on this paper is on DA
151 release by *Pseudo-nitzschia*, particulate DA along the drifter path data are not shown
152 but are the focus of a complementary paper by Lessard et al., (unpublished data).
153
154 *2.7. Pseudo-nitzschia cell counts and species identification*
155 Samples for cell quantification were collected at a nominal 1 m depth along the
156 Drifter A track using 10 L Niskin bottles. Total *Pseudo-nitzschia* cells were quantified
157 from whole water samples preserved with buffered formalin (<1% final concentration).
158 Cells were enumerated with a Palmer-Maloney counting chamber using a Zeiss
159 Axiovert 135 inverted light microscope. Samples (50 mL) were settled when necessary

for at least 24 h and counted at 200 x (total) magnification. Surface phytoplankton samples were collected for *Pseudo-nitzschia* species identification at each station using a 20-µm mesh phytoplankton net. *P. cuspidata* were positively identified using transmission electron microscopy (Lundholm et al., 2003).

Eutreptiella cell counts. Sub-samples for cell quantification were collected from the *Pseudo-nitzschia* sample bottles. Unpreserved, unstained *Eutreptiella* cells were quantified immediately using a Becton Dickenson FACSCalibur flow cytometer, equipped with a 15-mW laser exciting at 488 nm. Samples were run at a flow rate of 60 µL min^{-1} and the cells discriminated using particle size and chlorophyll content.

2.8. Sinking Rates

Samples for determination of sinking rates were collected from the surface (approximately, 1 m depth) using 10 L Niskin bottles. A modified SetCol (settling column) of Bienfang (1981) was used to estimate the sinking and floating rates of phytoplankton (Beall, 2009). Triplicate *ca.* 500 mL samples of the natural assemblage were homogenized and decanted into glass columns (2.6 cm diam., 50 cm tall). After a 3-h incubation, top, middle and bottom fractions were removed from the column. The volumes of the fractions were measured for each settling column. The rates estimated by the SetCol protocol were not sensitive to the fraction volumes as long as the top and bottom fractions range from 10% to 15% of the total volume in the column (Bienfang, 1981). The biomass in each fraction was determined by chlorophyll extraction using the same protocol as outlined previously. The sinking (ψ) and floating rates (A) were calculated by Equation 1.

$$A \text{ or } \psi = \frac{B_{frac(obs)} - B_{frac(pred)}}{B_{tot}} \left(\frac{h}{t}\right)$$

(Eq. 1)

where $B_{frac(obs)}$ is the observed biomass in the top (floating) or bottom (sinking) fractions. $B_{frac(pred)}$ is the predicted biomass of the fraction based on the sum of biomass in the column multiplied by the fraction volume relative to the total volume, h is the height of the column of water and t is the incubation time in hours.

2.9. Grow-out Incubation Studies

Seawater was collected every 2 days during the drift from a 5-10 m depth using a trace metal (TM) clean, all-Teflon® 'fish' pumping system that gently samples phytoplankton and microzooplankton (Wells et al., 2009). All experimental preparations were performed in a fabricated, positive pressure, all-plastic TM clean room using TM clean techniques. Seawater was filtered through a pre-rinsed 200-µm nylon mesh (Nitex®) to remove grazers and homogenized in a 50-L polypropylene carboy. Nutrient analysis was conducted on the initial seawater collected to determine if macronutrient additions were required and amended as necessary to achieve 15 µM nitrate, 2 µM orthophosphate, and 15 µM silicate at the beginning of the experiment. Trace metals had previously been removed from macronutrient stocks using a Chelex-100 ion exchange resin (Price et al., 1988; 1989). The thoroughly mixed seawater was dispensed into 250-mL clear, polycarbonate bottles before treatments were added. Treatments included amending the waters with iron ($FeCl_3$ additions of 1 or 3 nM), copper ($CuSO_4$ at 1 or 3 nM) or reducing the free iron through the addition of the chelator

desferrioximine (DFB) (Desferal® - as deferoxamine mesylate is N-[5-[3-[(5-aminopentyl)hydroxycarbamoyl]propionamido]pentyl]-3-[[5-(N-hydroxyacetamido)pentyl]carbamoyl]propionohydroxamic acid monomethanesulfonate) at 3 nM. The fully prepared bottles were placed in a clear Plexiglas® incubators. Temperature was maintained at sea-surface temperature with flowing surface seawater and the incident photosynthetic photon flux density (PPFD) reduced to an equivalent of ~50% of the maximum daytime irradiation using a combination of neutral density screening and blue Plexiglas®. Bottles were retrieved after four days (Day 4) and processed.

2.10. Photosynthetic Efficiency

Photosynthetic efficiencies were measured by comparing the photosynthesis vs. irradiance responses (P vs. E) on Days 0, 2, 4, and 6. Rates of photosynthesis derived from the amount of $NaH^{14}CO_3$ incorporated into the cells during short-term incubations in a temperature-controlled photosynthetron under controlled light intensities. Five-mL subsamples were dispensed into 20-mL clear glass scintillation vials and each vial was inoculated with 5 µCi of $NaH^{14}CO_3$. The vials were then strategically placed in a cool-white (halogen) light-field that provides PPFDs from 0 to 1,200 µmol photons m^{-2} s^{-1}. After incubation, subsamples were acidified with 0.5 mL of 10% HCl (v/v) to stop the reaction and allowed to degas for *ca.* 24 h prior to the addition of 15 mL of scintillation fluid (EcoLume™, MP Biomedicals LLC). Samples were subsequently mixed by gentle inversion and allowed to sit undisturbed in the dark until they were radio-assayed using liquid scintillation counting. All ^{14}C uptake (photosynthesis) rates were corrected for

dark uptake using the formula of Parsons et al. (1984), P-E curves generated using a non-linear, least-squares regression technique (KaleidaGraph©; Synergy Software). Rate estimates of photosynthesis, normalized to chlorophyll *a* were fitted to the 3-parameter P-E model of Platt and Gallegos (1980).

3. Results

During September of 2004, the Juan de Fuca eddy region experienced high densities of *Pseudo-nitzschia* spp. and the marine euglenoid, *Eutreptiella* sp. Lagrangian ARGOS-tracked drifters, deployed at the origin of the upwelled nutrients of the eddy, enabled us to continually track and sample the *Pseudo-nitzschia* bloom for seven days from its formation to demise. The most common species of *Pseudo-nitzschia* present was *P. cuspidata* that co-dominated the phytoplankton assemblage with the euglenoid, *Eutreptiella* sp.

This particular drifter was one of several deployed during September 2004 as part of a continuing evaluation of the surface current transport in the Strait of Juan de Fuca to Columbia River regions (McFadyen et al., 2005). Once deployed in the upwelled waters adjacent to the Juan de Fuca upwelling initiation site, the drifter proceeded to move northwest for three days then shifted south and circled towards the coastal waters often associated with the along-shore transport of the Columbia River (MacFadyen et al., 2005). Prior to exiting the eddy, the drifter movement slowed from drifter Day 4 to drifter Day 6 (Fig. 1). The short retention of the drifter corresponds to an approach to the coastal front, where the water mass had distinctly different temperature, salinity and nutrients. After drifter Day 6, the drifter continued moving in

a rapid pace southeast towards shore and was retrieved approximately 30 nautical miles offshore.

Biological and chemical measurements of the surface waters indicated that as the drifter proceeded through time and space, the sinuous path between drifter Day 5 and 6 corresponded to definable differences in water masses (Fig. 2). Water temperatures first declined and then increased, with the drifter experiencing moderately cooler, higher salinity waters on drifter Day 5 (Fig. 2A, 2B). From Days 1-4, total biomass (chl-*a*) increased then decreased, while nitrate and silicate concentrations increased slightly and the total densities of *Pseudo-nitzschia* spp. increased, then remained fairly constant (Fig. 3A-C). Inexplicably, the total abundance of *Pseudo-nitzschia* decreased 3-fold on Day 5 (Fig. 3C), without a corresponding decrease in biomass or drawdown of either nitrate or silicate (Fig. 3B). During the early days of the drifter-based observations, the loss of *Pseudo-nitzschia* cells from the surface waters was minimal. The cell sinking rates and the aggregation rates of *Pseudo-nitzschia* cells remained inconsequential, ensuring that the cells remained in the surface waters (Fig. 4) until the drifter and associated waters were impacted by the putative internal wave upwelling event on drifter Day 5 (details in Lessard et al., in prep.).

The most dramatic changes in the biology and chemistry occurred around drifter Day 5 associated with the cooler, higher salinity subsurface water signal (Figs. 2-3; drifter Days 6-8). After the exchange with the vertically mixed water mass there was a concurrent increase in cell aggregation (Fig. 4), a rapid increase in *Pseudo-nitzschia*-specific sinking rates, leading to a reduction in *Pseudo-nitzschia* cell density (Fig. 3C), and an unexpected but prominent increase in dDA concentrations (Figure 3D). Coincidentally, there was also a rapid drawdown of nitrate, but not silicate – indicating

a stimulated nutrient-drawdown by community members that did not include *Pseudo-nitzschia* or competing diatoms. Overall, total biomass was not reduced in the drifter days succeeding the transfer through the front. The most logical beneficiary of the change in water mass was the co-blooming euglenoid, *Eutreptiella* sp., that matched the cell densities of *Pseudo-nitzschia* for the first four drifter days (Lessard et al., in prep.).

In addition to the measurement of *Pseudo-nitzschia* density, macronutrient and DA concentrations, and the floating/sinking rates of *Pseudo-nitzschia*, the physiological "health" of the natural population was assessed using waters collected on Days 0, 2, 4 and 6 along the drifter path (Fig. 1). These waters were incubated for four days in deck-board incubators after amendment with Fe or Cu – elements that we propose influence the growth and DA-levels in *Pseudo-nitzschia*. The resulting photo-physiological "health" was assessed using the relative performance of the photosystem under increasing photosynthetic photon flux density (PPFD; Fig. 5). The photosynthetic rates, normalized to the concentration of *Pseudo-nitzschia* cells, were compared using ambient water supplemented with either 3 nM DFB or 3nM Cu + 3 nM DFB. Respectively, the enrichments allowed us to consider if the ambient waters were Fe-limited, Cu-limited, could be Fe-deplete and could be a combination of Fe-deplete but requiring Cu. We report the photo-physiological "health" of the community using the maximum rate of photosynthesis (P^b), estimated from the P vs. E curves for the natural phytoplankton community under natural conditions and then compared to amended conditions. For example, control (ambient) water collected on Day 0 (Fig. 5) achieved a maximum photosynthetic rate of *ca.* 4.5 µg C (µg chl *a*)$^{-1}$ h^{-1}. When these natural waters were amended with 3 nM DFB, creating Fe-stressed cells, the maximum photosynthetic rate decreased ~50%; whereas, when the Fe-stressed cells were also

299 supplemented with 3 nM Cu, the maximum photosynthetic rate was over 4-fold that of
300 the iron-stressed cells, and over 2-fold the rate of non-augmented cells.

301 Following this strategy, when cells along the drifter path were assessed for their
302 'photosynthetic health' (via assessment of the photo-physiological state) the early cells,
303 cells collected directly from the newly upwelled eddy waters, had a photosynthetic max
304 of 4 µg C (µg chl *a*)$^{-1}$ h^{-1} (Fig. 6), but the maximum photosynthetic rate dropped
305 dramatically to less than 2 µg C (µg chl *a*) h^{-1} for drifter Days 2 and 4. Supplementing
306 these waters with 3 nM Fe did not replenish the community's physiological deficiency.
307 However, by depleting the waters of available iron through the addition of DFB and
308 adding 3 nM Cu maximum photosynthetic rates of 8-11 µg C (µg chl *a*)$^{-1}$ h^{-1} were
309 achieved.

310 In the second phase of the drifter path, when high salinity, low temperature
311 waters altered the character of the surface waters (drifter Days 6-7; Fig. 2), the
312 physiological response of the community changed dramatically. The community
313 achieved greater maximum photosynthetic rates, with values approaching 7 µg C (µg
314 chl *a*)$^{-1}$ h^{-1} (Fig. 6). Supplementing the community with 3 nM Fe neither increased nor
315 decreased the photosynthetic capacity. However, the amendment of the Fe-enriched
316 sample with 3 nM Cu depressed the maximum photosynthetic capacity to < 1 µg C (µg
317 chl *a*)$^{-1}$ h^{-1} – a reduction of rates that indicate Cu-toxicity.

318 To assess the impact of Cu and Fe additions, or Fe removal by DFB enrichment,
319 1 or 3 nM of either Fe, Cu, DFB or DFB + Cu were added to the grow-out incubation
320 bottles, and cell growth and toxin characteristics were assessed after 4 days of deck-
321 board incubation. At all stations, the addition of Fe-stimulated biomass proportional to

the level of Fe added – indicative of some degree of Fe limitation. In contrast, the addition of Cu reduced the achieved biomass. The increase in biomass was positively related to the concentration of added Fe (Fig. 7A). There was a corresponding reduction in achieved biomass under all other treatments for drifter Days 0, 2, and 4. The community from drifter Day 6 showed no significant difference in growth compared with the control (open bars) when provided Cu, DFB or DFB + Cu (Fig. 7B-D).

Considering that the treatments may not affect all genera in a similar fashion, the concentrations of *Pseudo-nitzschia* were recorded over the 4-day incubation period. Generally, *Pseudo-nitzschia* was stimulated by all treatments, in particular after drifter Day 0 (Fig. 8). The most dramatic stimulation of *Pseudo-nitzschia* growth occurred on drifter Day 4, particularly when DFB was added, alone or in combination with Cu (Figure 8B, D), whereas the *Pseudo-nitzschia* population from drifter Day 6 responded weakly to all treatments.

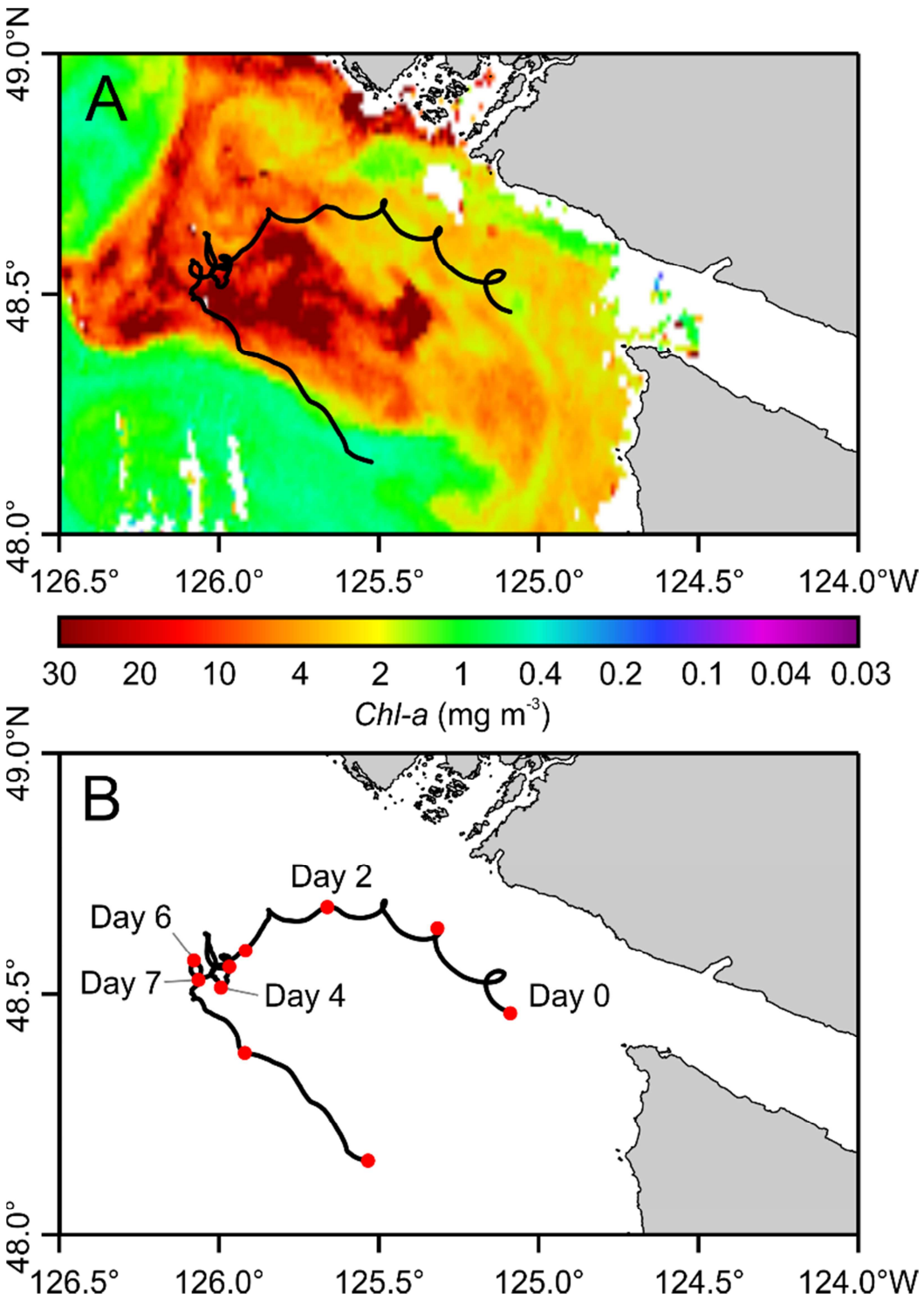
A
49.0°N
48.5°
48.0°
126.5°
126.0°
125.5°
125.0°
124.5°
124.0°W
30
20
10
4
2
1
0.4
0.2
0.1
0.04
0.03
Chl-a (mg m-3)
B
Day 2
Day 6
Day 7
Day 4
Day 0

340 **Figure 1**. Path of the drifter in the Juan de Fuca Eddy during ECOHAB-PNW-III
341 Cruise: **A.** An overlay of the drifter path over a SeaWIFS image of the Juan de Fuca
342 eddy region image taken Day 3 (September 19, 2004). **B.** The track of drifter. The
343 drifter was placed in the central edge of the eddy on Day 0. Samples for the data
344 presented here were collected at the indicated locations as red circles (●) using either a
345 10 L Niskin bottles or using the trace metal clean 'fish' and pump sampler.
346

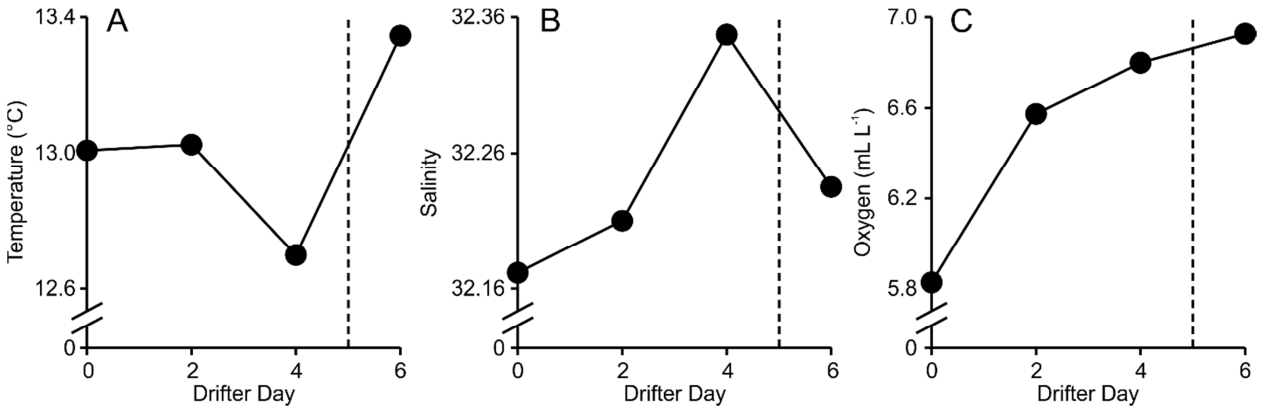

Figure 2. Physical and chemical parameters measured on Days 0, 2, 4, and 6, corresponding to the dates of the grow-out experiments, along the drifter path in the Juan de Fuca Eddy, September 2004. Discrete samples were collected using 10-L Niskin bottles and processed on board. The dashed line at Day 5 signifies entry into the second phase of the drifter path.

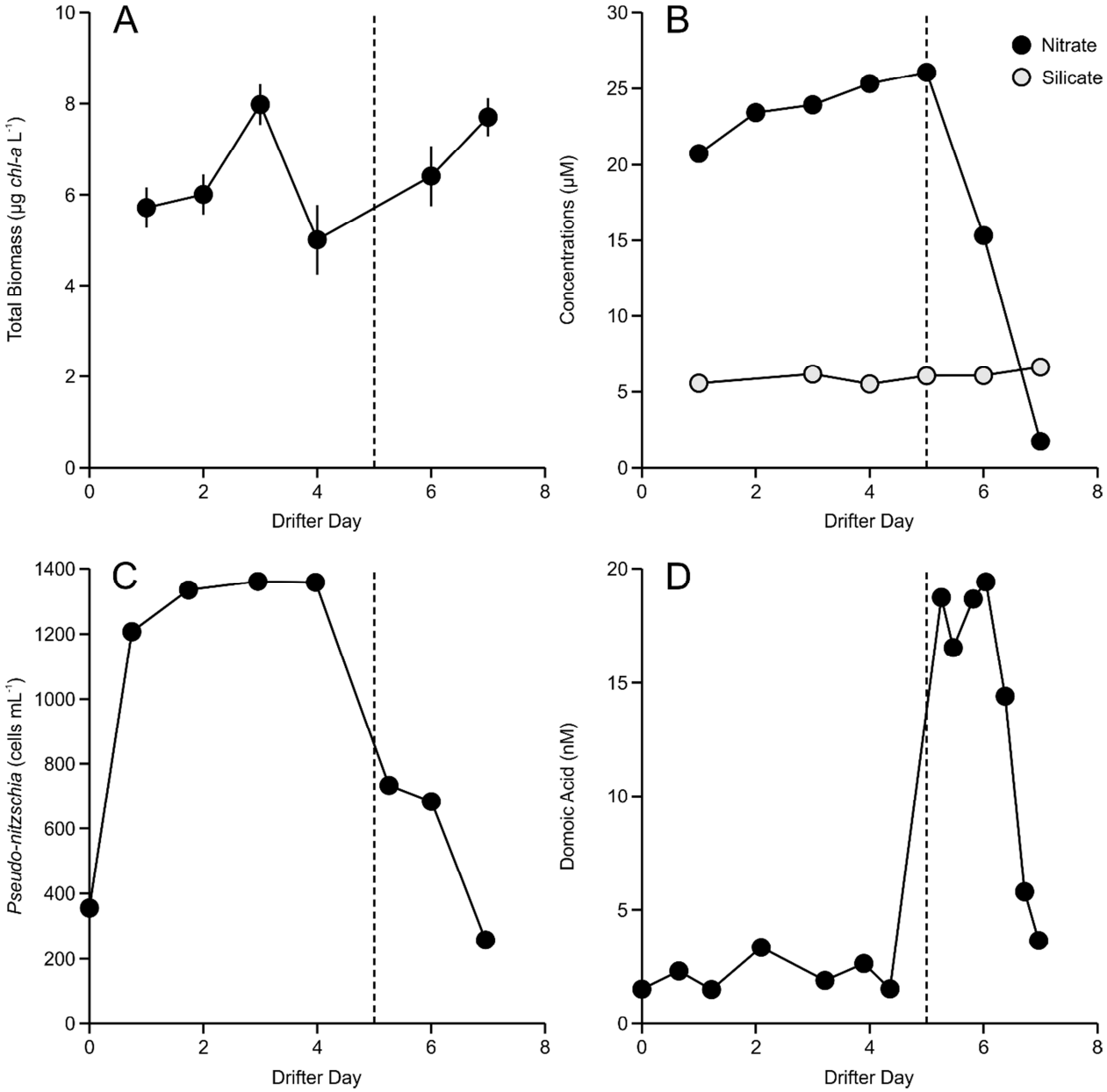

357
358

359 **Figure 3.** Development of the A) phytoplankton biomass (extracted chlorophyll *a*) (n =
360 2, range reported), B) nitrate and silicate concentrations, C) Surface *Pseudo-nitzschia*
361 concentrations and D) Surface dissolved DA during the drifter path in the Juan de Fuca
362 Eddy in September 2004. Samples were collected using 10 L Niskin bottles. The
363 dashed lines signify entry into the second phase of the drifter path after Day 5.

364

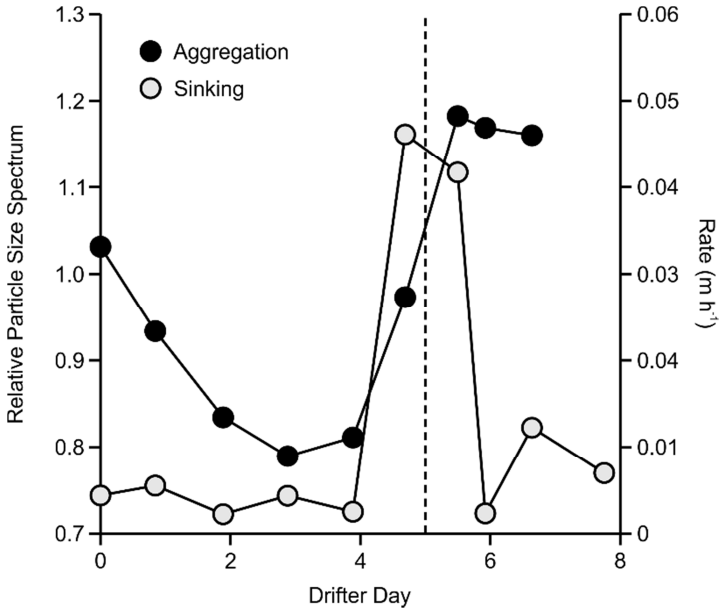

Figure 4. Phytoplankton community sinking rates (○) and aggregation (floating; ●) rates in the mixed layer (5 m depth) during the Juan de Fuca drifter experiment in September 2004. Samples were collected at the 5-m using 10 L Niskin bottles. The dashed lines signify entry into the second phase of the drifter path after Day 5.

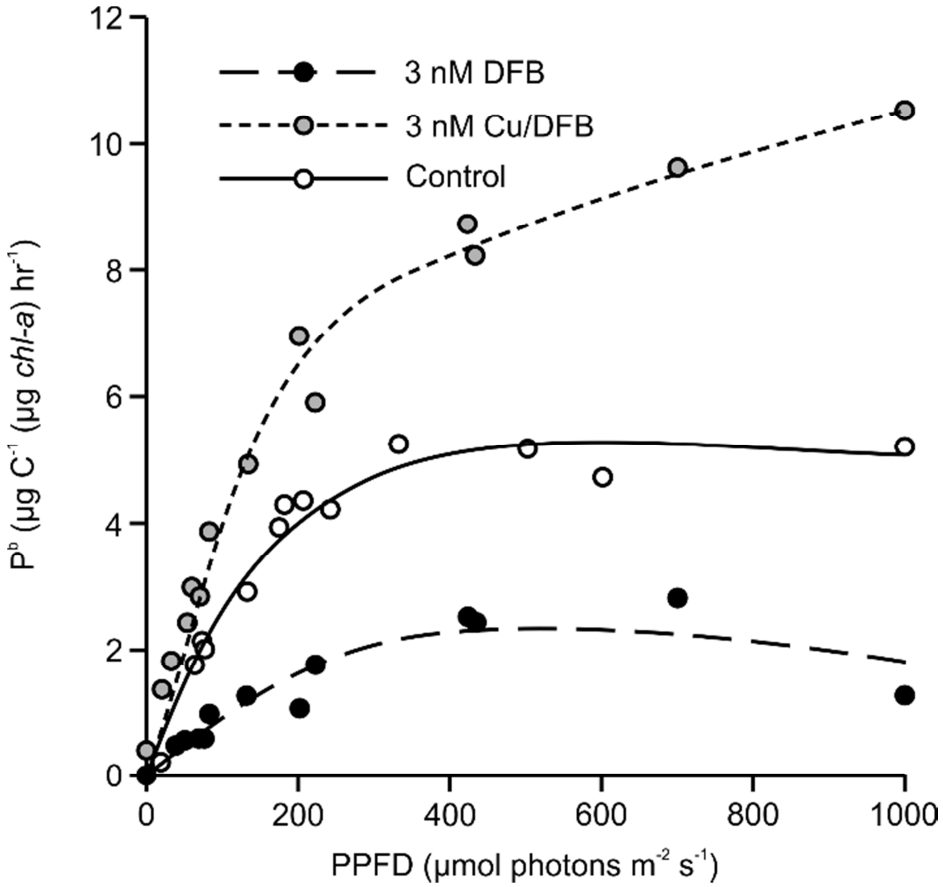

Figure 5. Effects of 3 nM desferoxamine (DFB) and 3 nM Cu additions on the photosynthetic capacity of natural phytoplankton communities as a function of photosynthetic photon flux density (PPFD). All samples collected from drifter Day 0 using the trace metal clean fish. The control represents photosynthetic rates from un-amended waters.

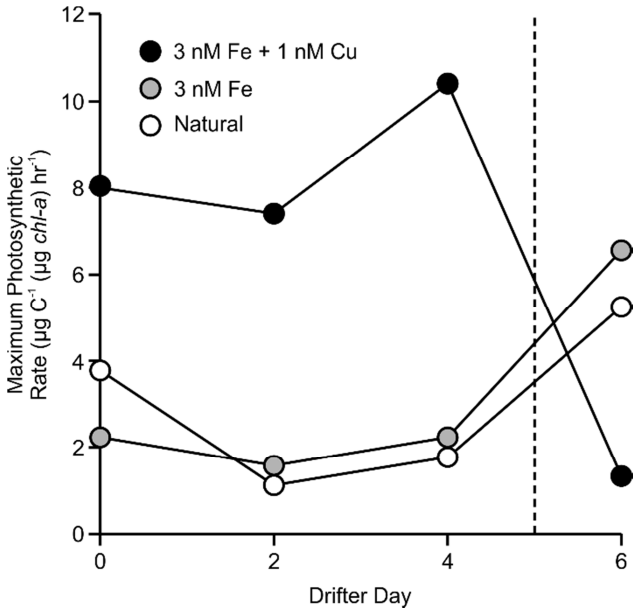

Figure 6. Effects of Fe and Cu additions on the maximum photosynthetic rates of cells collected on Days 0, 2, 4, and 6 along the drifter path using the trace metal clean fish. The combination of Fe + Cu addition enhanced the photosynthetic performance in the *Pseudo-nitzschia* dominated early stages of the drifter path, whereas, the phytoplankton community from the sample stations after drifter Day 4 were highly sensitive to trace metal additions. Natural samples are unamended waters. The dashed lines signify entry into the second phase of the drifter path after Day 5.

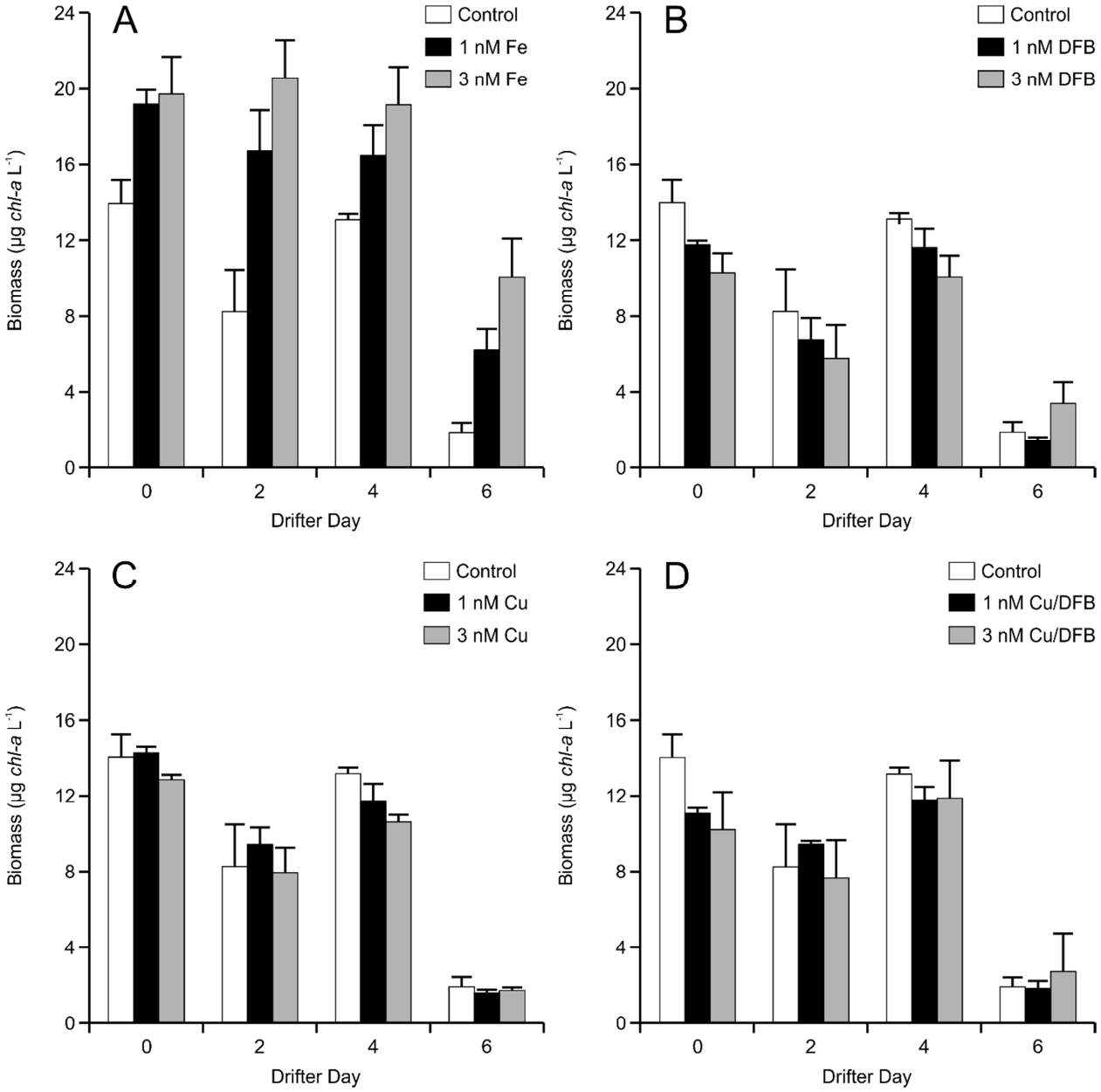

394
395

396 **Figure 7.** Responses of phytoplankton biomass measured after 4-day deck-board 'grow-
397 out' incubations of ambient water collected using the trace metal clean fish on Days 0,
398 2, 4, and 6 along the drifter path in the Juan de Fuca Eddy, September 2004. Duplicate
399 bottles were supplemented with macronutrients, then further supplemented with either
400 A) iron, B) desferoxamine (DFB), C) copper, and D) copper + DFB. Bars show the
401 range of responses (n=2).

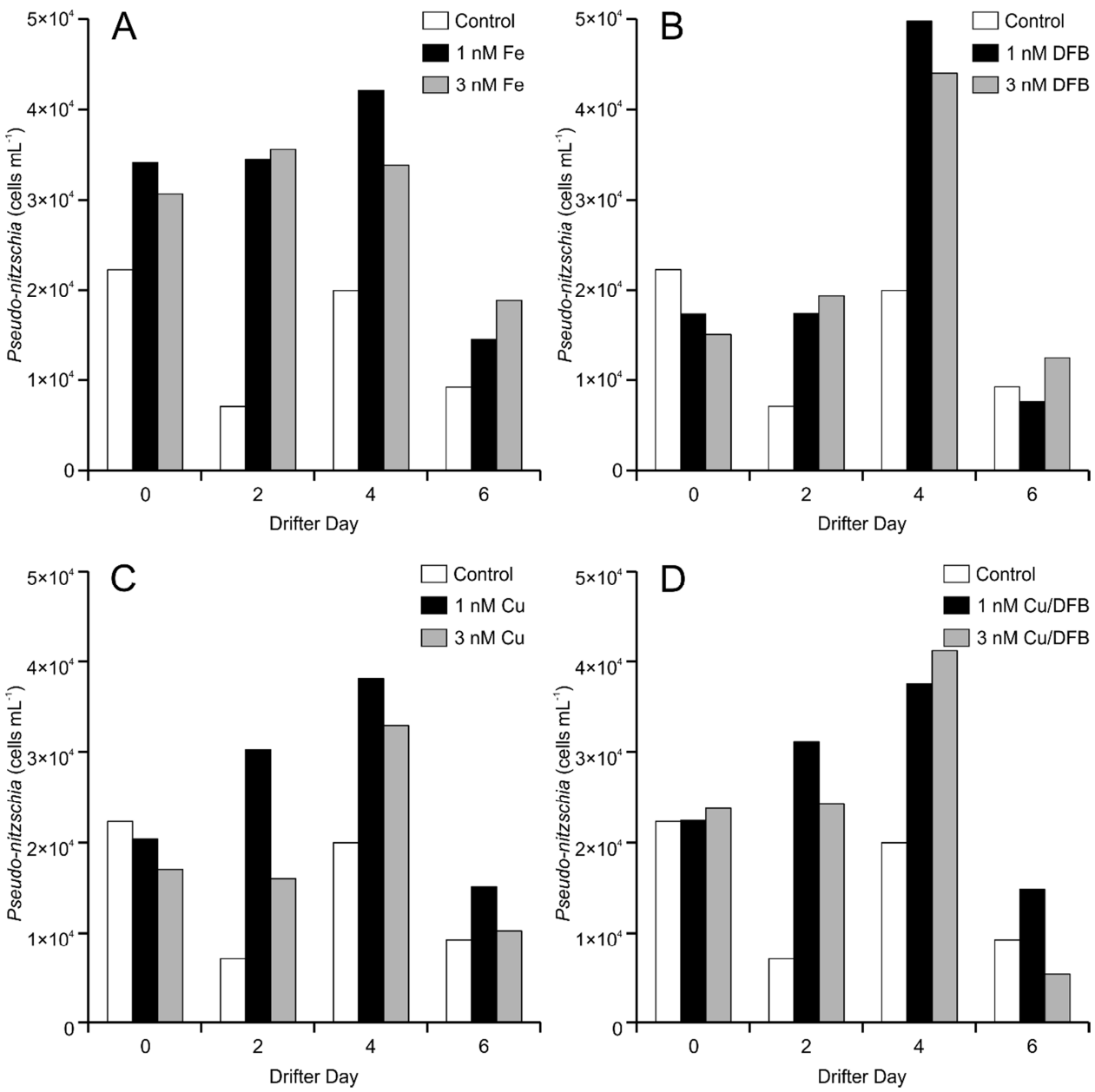

Figure 8. The growth response of *Pseudo-nitzschia* after 4-day 'grow-out' incubations of ambient water collected using the trace metal clean fish on Days 0, 2, 4, and 6 along the drifter path in the Juan de Fuca Eddy, September 2004. Bottles were supplemented with indicated macronutrients, and with either: A) iron, B) desferoxamine (DFB), C) copper, and D) copper + DFB. Single samples were analyzed.

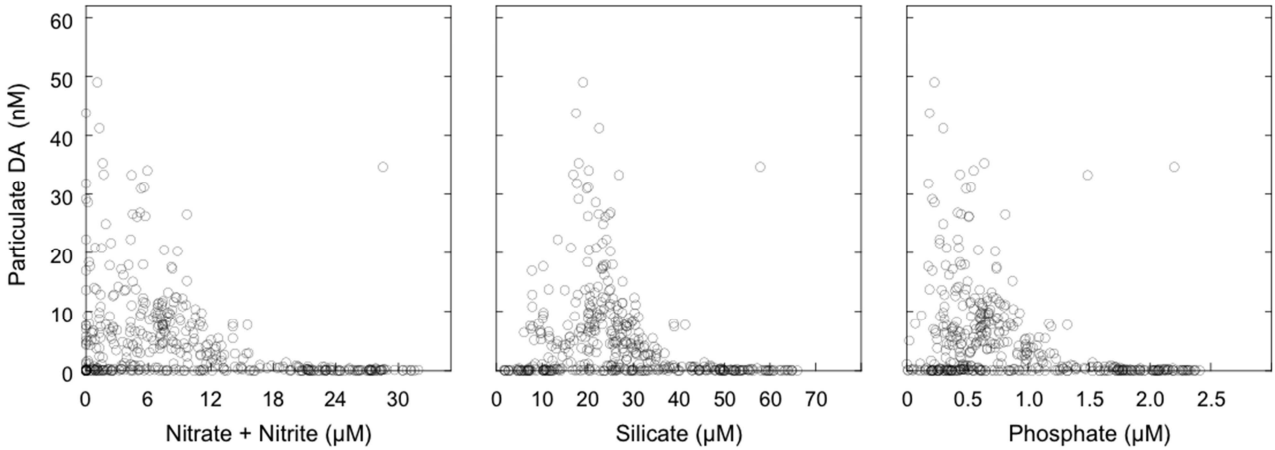

411

412 **Figure 9**. *In situ* concentrations of particulate DA (pDA) verses ambient concentrations

413 of nitrate plus nitrite, silicate, and phosphate of surface waters during the ECOHAB-

414 PNW-III Cruise in September 2004 (data from Trainer et al., 2009).

415

4. Discussion

The Juan de Fuca Eddy off Vancouver Island, British Columbia, Canada and the Washington coast, USA was reported by Trainer et al. (2009a, b) to contain a large, nearly monospecific diatom bloom of *P. cuspidata* in September 2004 that also contained the euglenoid, *Eutreptiella* spp. *Pseudo-nitzschia cuspidata* reached cell densities of ~ 6.1 x 10^6 cells L^{-1} and produced maximum particulate domoic acid (pDA), dissolved domoic acid (dDA), and cellular domoic acid concentrations of 43 nmol L^{-1}, 4 nmol L^{-1}, and 63 pg $cell^{-1}$, respectively. The synoptic survey conducted during this time revealed that 84% of the stations (n = 598) had detectable *Pseudo-nitzschia* cells and 78% had detectable levels of pDA. Variable ratios of pDA:dDA in the eddy region suggested that DA release was under cellular regulation by *Pseudo-nitzschia*, however, there were no significant correlations between either pDA or cellular DA and ambient concentrations of macronutrients, including silicate (Figure 9). Even so, pDA in surface waters (1-5 m depth) was positively correlated with chl *a* and negatively correlated with temperature ($p < 0.01$) when *Pseudo-nitzschia* was present. These findings demonstrate that Si limitation is not a prerequisite or 'trigger' for *Pseudo-nitzschia* toxicity, as is commonly stated (e.g., Du et al., 2016), and that the mechanistic basis for DA synthesis is linked instead to other environmental or nutritional factors. Similarly, there were no significant correlations between cellular DA concentrations and planktonic bacteria or cyanobacteria abundances (Beall, 2009), contrary to the purported links between bacteria activity and DA production by *Pseudo-nitzschia* (cf., review by Lelong et al. 2014), although we cannot rule out that there may have been significant changes in the composition of the bacterial community (e.g.,

439 Hattenrath-Lehmann and Gobler, 2017) or that bacteria comprising the biofilm of
440 natural eukaryotic cell walls may contribute to DA production. There was a correlation
441 between limiting concentrations of Fe (*ca.* 0.1 nmol L^{-1}) and the greatest *Pseudo-*
442 *nitzschia* abundances, as well as pDA and dDA concentrations (Trainer et al., 2009a, b).
443 The study here focused on a single drifter deployment during the synoptic
444 survey described by Trainer et al. (2009a) where the oceanographic and physiological
445 conditions of a surface population of *Pseudo-nitzschia* were tracked over time within
446 the Juan de Fuca Eddy system. The drifter faithfully followed a single patch of surface
447 water over six days before being ejected in a southeast direction across the perimeter of
448 the eddy core on Day 7, requiring 2 more days to be ejected completely from the eddy
449 into the coastal current (Lessard et al., in prep.). Internal wave forcing within this
450 dynamic system generated periodic infusions of colder, more saline, subsurface waters
451 into the surface patch (Fig. 2), which would have resupplied it with nutrients. Here, our
452 findings can be viewed in terms of a natural "semi-continuous batch" culture system,
453 where the phytoplankton community in the advected surface patch was supported by at
454 least two nutrient re-infusions over the 6-day circumnavigation of the eddy core (Fig.
455 3).
456 The periodic vertical infusion of subsurface water helps to explain the rather
457 sluggish changes in dissolved macronutrient concentrations that accompanied the small
458 but marked increases in total biomass and significant increases in *Pseudo-nitzschia*
459 abundance (Fig. 3). There was no net consumption of nitrate, silicate, and phosphate
460 (data not shown) over this period, and indeed nitrate concentrations actually increased
461 as the bloom developed (Fig 3B). The combination of a persistently elevated *Pseudo-*
462 *nitzschia* abundance (Fig 3C), stable photosynthetic rates (Fig. 6), and low sinking rates

463 (Fig. 4), all point to the maintenance of a healthy phytoplankton community over the
464 first 4 days. Indeed, the initially elevated rates of aggregation and lower cell abundance
465 on Day 0 suggest that the *Pseudo-nitzschia* community had re-emerged from less
466 favorable pre-drifter conditions, perhaps stimulated by vertically-advected infusion of
467 subsurface waters prior to sampling and Day 1 (Fig. 1).

468 *Pseudo-nitzschia* cell densities declined precipitously between Days 4 and 5
469 (Fig. 3c), signaling the collapse of the bloom. The onset of this collapse was not closely
470 related to declining macronutrient concentrations, which occurred after Day 5. Bloom
471 termination corresponded closely with the intensification of *Pseudo-nitzschia*-cell-
472 specific sinking rates (Fig. 4) and the order of magnitude increase in dissolved DA
473 concentrations (*ca.* 2 to 20 nM dDA) in surface waters (Fig. 4D). Nonetheless, rapid
474 declines in *Pseudo-nitzschia* abundance after Day 4 had little effect on total
475 (chlorophyll) biomass (Fig 3A) due to the compensatory increase in the abundance of
476 the marine euglenoid, *Eutreptiella* (Lessard et al., in prep.).

477 The factor, or factors, causing the transition from a *Pseudo-nitzschia*- to
478 *Eutreptiella*-dominated community after Day 4 are not known. There is no indication
479 that increased grazing pressure was responsible (Lessard et al., in prep.). And the
480 collapse of the *Pseudo-nitzschia* bloom clearly was not triggered by limiting
481 concentrations of nitrate, silicate, or phosphate; the acute drop in nitrate concentrations
482 occurred between Days 5 and 6, after the decline in *Pseudo-nitzschia* began, and even
483 on Day 6, nitrate concentrations were still in excess of those required to support
484 maximum rates of uptake by cells of the *P. pseudodelicatissima* complex (Auro and
485 Cochlan, 2013). This is in contrast with prior, largely stable nutrient conditions,
486 suggesting that nutrient infusion from internal wave processes ceased, consistent with

the physical data (Fig. 2). Despite the rapid decrease in *Pseudo-nitzschia* abundance there were only marginal if any change in total biomass (Fig. 3b), attributable to further in-growth of *Eutreptiella* spp. (Lessard et al., in prep.). The enhanced growth of *Eutreptiella* within the community coincides with a roughly 3-fold increase in photosynthetic capacity of the transitioning community (Fig 6) and the relaxing of the iron-limitation of the community. The absence of comparable silicate drawdown (Fig. 3b) is further evidence of the declining health of *Pseudo-nitzschia* during this transition.

If not decreased availability of macronutrients, what then could have initiated the collapse of the *Pseudo-nitzschia* bloom? It is feasible that the transition was associated with some degree of lateral advection of "patchy" surface waters, given the dynamics of this system, however, the survey data showed reasonable spatial uniformity in the composition of surface water phytoplankton community (Trainer et al., 2009a). At best, any lateral advection would have accelerated the apparent community transition that was occurring more broadly in the region.

The deck-board incubation experiments demonstrate that the community was Fe stressed, with the Fe treatment generating markedly greater total biomass (Fig 7a) and *Pseudo-nitzschia* abundance (Fig. 8a) over the course of the drifter study. The same was true immediately outside the core perimeter of the Eddy on Day 6 (Fig. 7a). Importantly Fe amendments did not enhance cell photophysiology (Fig. 6) however, indicating that there was sufficient Fe availability in the surface waters to maintain the existing community, but that more Fe was needed to enable further biomass accumulation. Even so, the abnormally elevated dissolved DA concentrations (*ca.* 2-3 nM) are consistent with *Pseudo-nitzschia* experiencing significant Fe stress (Maldonado et al., 2002; Wells et al., 2005).

511 Further evidence that there was insufficient biologically-available Fe during the
512 drifter bloom is the comparative ease that Fe stress could be induced by adding the
513 siderophore DFB. Additions of DFB to both laboratory cultures and natural
514 phytoplankton communities can decrease Fe availability (Hutchins et al., 1999; Wells,
515 1999; Wells and Trick, 2004, Shaked and Lis, 2012), and the same decreasing trend in
516 achieved total biomass with progressively greater siderophore concentrations was seen
517 here (Fig. 7b). The increased Fe stress is seen in the lowered community photosynthetic
518 capacity in the DFB- amended incubations (Fig. 5). Although dissolved Fe
519 concentrations were not measured during the cruise, previous experience in the region
520 suggested that 1-3 nM DFB additions would complex 'some-to-much' of the dissolved
521 Fe pool, through ligand exchange with the natural organic ligands (Rue and Bruland,
522 2001). But trace metal determinations during three subsequent cruises to this region
523 showed Fe concentrations of *ca.* 2-5 nM Fe (Roy, 2009), so it is reasonable to expect
524 that the DFB amendments would have been sufficient to complex much but perhaps not
525 all of the ambient dissolved Fe. This perspective is in agreement with the somewhat
526 muted impact of DFB on total biomass accumulation (Fig. 7B). In summary, the
527 phytoplankton community was Fe-stressed at the start and over the 6-day drifter
528 experiment, with biomass increasing upon Fe addition, and decreasing when a portion
529 of the ambient pool of Fe was made less available by complexation with DFB.
530 DFB amendments led to a decreased abundance of *Pseudo-nitzschia* in the deck-
531 board incubations during the early phases of the bloom (Days 2 & 4), but this effect was
532 vividly reversed on Day 6, when *Pseudo-nitzschia* abundance increased sharply in the
533 DFB treatment (Fig. 8a, b). This reversal coincided with onset of the bloom decline in
534 surface waters (Fig. 3C), and the order of magnitude increase in dissolved DA

concentrations (Fig. 3D). So, when the deck-board incubation was started on Day 6, DA concentrations were > 5-fold in excess of the added DFB concentration. Although DA complexes Fe in seawater (Rue and Bruland, 2001), it still would not have competed effectively with DFB for Fe given the massive difference in their conditional stability constants in seawater ($logK^{cond}_{FeDA,Fe(III)'}$= $10^{8.7\pm0.5}$ M^{-1} vs. $logK^{cond}_{FeDFB,Fe(III)'}$= $10^{16.5}$, Rue and Bruland, 1995, 2001). It is likely instead that the increased dDA concentrations signal physiological impacts on *Pseudo-nitzschia* associated with the increased Fe stress caused by DFB. A similar response has been shown in culture when *Pseudo-nitzschia* spp. are placed under Fe limiting conditions (Wells et al., 2005).

P. multiseries and *P. australis* can fulfil their Fe growth requirements for rapid exponential growth when non-complexed dissolved Fe concentrations (Fe') are greater than ~ 25 pM (Maldonado et al., 2002), and it is reasonable to anticipate that *P. cuspidata* would not have substantially different requirements. The bulk dissolved Fe concentrations in these waters would be in far excess of this oceanic level (Roy, 2009), meaning that the vast bulk of dissolved Fe in the drifting patch existed in organically complexed forms that were not easily available to *P. cuspidata* (Trick et al., 2004). Although *Pseudo-nitzschia* sp. appear to be less efficient at Fe uptake than other diatoms under Fe-replete conditions, experiments demonstrate their superior ability to adapt under Fe deplete conditions (Maldonado et al., 2002; Wells et al., 2005), and that the production and release of DA facilitates Fe acquisition and alleviating Fe stress. This enhanced Fe acquisition appears to result from *Pseudo-nitzschia* being able to directly extract Fe from strong Fe complexes, as long as Cu is readily available (Maldonado et al., 2002 Wells et al., 2005). Other diatoms also show a Cu requirement

for enhanced Fe uptake under Fe stressed conditions, along with reduced Fe requirements through substitution for Fe-containing enzymes in the photosynthetic transport chain (Grotz and Guerinot, 2006; Nouet et al., 2011). Here, Cu amendment had little to no consistent effect on total biomass, yielding only slight decreases at the highest Cu addition (3 nM) on Days 2 and 4 (Fig. 7C). However, adding Cu sharply stimulated *Pseudo-nitzschia* growth within the community (Fig 8C) when *Pseudo-nitzschia* abundance was high (Fig 3C). The same result has been observed in cultures under Fe stress conditions (Maldonado et al., 2002; Wells et al., 2005).

The addition of Cu with DFB enhanced *Pseudo-nitzschia* growth during the earlier phase of the bloom by 30-45% over that observed in the DFB only treatment (Fig. 8C, D). This effect was even more clearly shown in the photo-physiological measurements of the *in-situ* assemblage, where addition of Cu with DFB reversed the negative effect of DFB alone (Fig. 5); indeed, the combination of DFB and Cu yielded a higher photosynthetic capacity than the control. However, these positive effects were reversed in the incubation initiated on Day 5, when the collapse of the bloom had begun, where the combination of decreased Fe availability and increased Cu additions led to markedly lower *Pseudo-nitzschia* growth. It may be that the decreases in health of the *Pseudo-nitzschia* population, as shown by the increased aggregation, sinking rates, and photo-physiology, were sufficiently massive to prevent recovery.

The substantial increase in dDA at the end of the bloom would not have substantially affected dissolved Fe speciation. Rue and Bruland (2001) calculate that dDA concentrations of 100 nM would lead to DA complexation of *ca.* 25% of the dissolved Fe pool, so by extrapolation only *ca.* 5% of Fe would have existed as a DA complex in the drifter surface waters. However, the DA release would have affected

582 dissolved Cu speciation to a much greater extent, reducing free cupric ion
583 concentrations by a factor of 2-3 during Days 0-4, and by more than a 100-fold after
584 Day 5 (Rue and Bruland, 2001). Given the combined observations showing targeted
585 release of DA by Fe-starved *Pseudo-nitzschia*, it's strong effect on Cu complexation,
586 the positive Cu effect on *Pseudo-nitzschia* photo-physiology (Fig. 5), and the necessity
587 of Cu for enhancing growth of Fe-stressed *Pseudo-nitzschia* in both the laboratory
588 (Maldonado et al., 2002; Wells et al., 2005) and field conditions (Wells et al., 2005; Fig.
589 8C), we believe that DA production affects the ecophysiology and success of *Pseudo-*
590 *nitzschia* in coastal waters through the alleviation of Fe limitation via enhanced Cu
591 acquisition.

592 The sharp increase in dDA concentrations coincided with the transition from a
593 *Pseudo-nitzschia*-dominated to a *Eutreptiella*-dominated community. *Pseudo-nitzschia*
594 spp. appear to be somewhat more sensitive to Cu toxicity than other diatoms
595 (Maldonado et al., 2002), and one might hypothesize that the purpose of DA release by
596 the cell is to diminish Cu toxicity, were it not for the observations that Cu is essential
597 for inducing the high affinity Fe uptake system in *Pseudo-nitzschia* (Wells et al., 2005).
598 Although we have no direct measure of the sensitivity of the co-occurring *Eutreptiella*
599 spp. to Cu, other euglenoids show significant sensitivity (Netto et al., 2012). It seems
600 possible then that decreases in cupric ion concentrations due to the large release of
601 dissolved DA during the collapse of the *Pseudo-nitzschia* bloom may have enhanced the
602 growth success of *Eutreptiella*.

603 Nitrogen measurements on the cruise were limited to oxidized N forms, so we
604 are unable to assess whether DA production was related to changes in the supply of
605 reduced nitrogen forms, even though we now know that the form of nitrogen is critical

to DA production (Howard, et al., 2007; Radan and Cochlan, 2018).

5. Conclusions

The rapid response to additions of Cu and Fe - leading to increased biomass – changes that are catalysed with the release of dDA, illustrate why simple correlations between dDA and environmental conditions, such as with macronutrient concentrations, have not revealed a strong association. Our multi-day investigation of bloom progression illustrates that the rapid release of dDA is highest at the intersection of three critical conditions (sufficient macronutrients, low Fe and low Cu). Our corresponding survey approach never revealed the intensive release of dDA under these conditions. The lack of reveal is due potentially to the rapid response of the cells to altered environmental condition, and the ephemeral nature of the three conditions in the waters of the PNW. Typical static cruise sampling protocols where the time (distance) between sampling locations are long lack to precision to capture the toxin signal. This work adds supporting evidence to the important role of trace metals, not macronutrient limitation (most notably silicate) in forecasting the success and demise of toxigenic *Pseudo-nitzschia* in the PNW. Although the toxic threat of DA to coastal ecosystems and the health of marine mammals, birds and humans, is directly linked to the concentration of particulate DA (pDA). The present study clearly underscores the physiological importance of dissolved DA in the development of such toxic diatom blooms. It is not just a wicked problem, but a wickedly transient problem.

Acknowledgements. This research was part of The Ecology and Oceanography in the Pacific Northwest (ECOHAB-PNW) project supported by the National Science

630 Foundation ECOHAB project OCE-0234587, and National Oceanic and Atmospheric
631 Administration ECOHAB grant NA16OP1450 awarded to VLT, WPC, and MLW, and
632 a NSERC Discovery grant to CGT. We appreciate the skill and professionalism of the
633 Captain and crew of the R/V *Atlantis.* They ensured that we were able to follow the
634 drifters - in spite of the ship traffic at times. We acknowledge and thank J. Herndon
635 (SFSU) for nutrient and chlorophyll analysis, B. Bill (NOAA) for the *Pseudo-*
636 *nitzschia* cell enumeration, K. Baugh and S. Nance (NOAA) for DA analyses, Liza
637 Barney (WU; née McClintock) and Nick Ladizinki (SFSU) for flow cytometry and P vs
638 E measurements, N. Kachel (UW) for conductivity, temperature, depth (CTD) analyses,
639 B. Hickey, S. Geier (UW) and numerous other colleagues for cruise support. N. Adams
640 and D. Aldred creatively prepared the figures. This is ECOHAB publication ECO926
641 and ECOHAB-PNW publication #36."

642

643 **Author Contributions.** All authors contributed to study design, sample acquisition,
644 experimental manipulations, and interpretation of results; all authors contributed to the
645 manuscript.

646
647 **Competing Financial Interests statement:** The authors declared no competing
648 interests.

649 **References**

650 Adams, N.G., Lesoing, M., Trainer, V.L., 2000. Environmental conditions associated with
651 domoic acid in razor clams on the Washington coast. J. Shellfish Res. 19, 1007-1015.

652 Auro, M.E., Cochlan, W.P., 2013. Nitrogen utilization and toxin production by two
653 diatoms of the *Pseudo-nitzschia pseudodelicatissima* complex: *P. cuspidata* and *P.*
654 *fryxelliana.* J. Phycol. 49, 156-169.
655 Beall. B.F.N., 2009. Studying plankton community dynamics in the subarctic Pacific
656 Ocean using flow cytometry. Ph.D. Thesis, Western University, London, Ontario. 196p.
657 Bienfang, P., 1981. SETCOL — A technologically simple and reliable method for
658 measuring phytoplankton sinking rates. Can. J. Fish. Aquat. Sci., 38, 1289-1294.
659 Bill, B.D., Cox, F.H., Horner, R.A., Borchert, J.A., Trainer, V.L., 2006. The first closure
660 of shellfish harvesting due to domoic acid in Puget Sound, Washington, USA. Afr. J. Mar.
661 Sci. 28, 435–440.
662 Chadsey, M., Trainer, V.L. Leschine, T.M., 2011. Cooperation of science and
663 management for harmful algal blooms: domoic acid and the Washington coast razor
664 clam fishery. Coastal Manage. 40, 33-54.
665 Davis, R. 1985. Drifter observations of coastal surface currents during CODE: The
666 method and descriptive view. J. Geophys. Res., 90, 4756-72.
667 Du, X., Peterson, W., Fisher, J., Hunter, M., Peterson, J. 2016. Initiation and
668 development of a toxic and persistent *Pseudo-nitzschia* bloom off the Oregon coast in
669 spring/summer 2015. PLoS One 11(10), e0163977.
670 Dyson, K., Huppert, D.D. 2010. Regional economic impacts of razor clam beach
671 closures due to harmful algal blooms (HABs) on the Pacific coast of Washington.
672 Harmful Algae 9, 264-271.

673 Garthwaite, I., Ross, K.M., Miles, C.O., Hansen, R.P., Foster, D., Wilkins, A.L.,
674 Towers, N.R. 1998. Polyclonal antibodies to domoic acid, and their use in
675 immunoassays for domoic acid in sea water and shellfish. Nat. Toxins 6: 93–104.

676 Gordon, H.R., Wang, M. 1994. Retrieval of water-leaving radiance and aerosol optical
677 thickness over the oceans with SeaWiFS: a preliminary algorithm. Appl. Opt. 33, 443-
678 452.

679 Grotz, M., Guerinot, M.L. 2006. Molecular aspects of Cu, Fe and Zn homeostasis in
680 plants. Biochim. Biophys. Acta – Mol. Cell Res. 1763, 595-608.

681 Hattenrath-Lehmann, T., Gobler, C.J. 2017. Identification of unique microbiomes
682 associated with harmful algal blooms caused by Al*exandrium fundyense* and *Dinophysis*
683 *acuminate*. Harmful Algae 68, 17-30

684 Hickey, B., MacFadyen, A., Cochlan, W.P., Kudela, R., Bruland, K., Trick, C.G. 2006.
685 Evolution of chemical, biological and physical water properties in the northern
686 California current in 2005: Remote or local wind forcing? *Geophysical Research Letters*
687 33(L22S02): doi:10.1029/2006GL026782.

688 Hickey, B.M., Trainer, V.L., Kosro, P.M., Adams, N.G., Connolly, T.P, Kachel, N.B.,
689 Geier, S.L. 2013. A springtime source of toxic *Pseudo-nitzschia* cells on razor clam
690 beaches in the Pacific Northwest. Harmful Algae 25, 1-14.

691 Howard, M. D. A., Cochlan, W. P., Ladizinsky,N., Kudela, R.M. 2007. Nitrogenous
692 preference of toxigenic *Pseudo-nitzschia australis* (Bacillariophyceae) from field and
693 laboratory experiments. Harmful Algae 6, 206-217.

694 Hutchins, D.A., Witter, A.E., Butler, A., Luther, G.W. 1999. Competition among marine
695 phytoplankton for different chelated iron species. Nature 400, 858–861.

696 Knepel, K., Bogren, K., 2002. Determination of orthophosphate by flow injection
697 analysis: QuikChem®Method 31-115-01-1-H. Lachat Instruments, Milwaukee, WI, 14 pp.

698 Lelong, A., Hégaret, H., Soudant, P. 2014. Link between domoic acid production and cell
699 physiology after exchange of bacterial communities between toxic *Pseudo-nitzschia*
700 *multiseries* and non-toxic *Pseudo-nitzschia delicatissima*. *Marine Drugs* 12, 3587–3607.

701 Lessard, E.J. et al., in prep. Evolution of an extensive toxic *Pseudo-nitzschia cuspidata* and
702 *Eutreptiella cf. gymnastica* bloom originating in the Juan de Fuca Eddy: a Lagrangian study.

703 Lewitus, A.J., Horner, R.A., Caron, D.A., Garcia-Mendoza, E., Hickey, B.M., Hunter, M.,
704 Huppert, D.D., Kudela, R.M., Langlois, G.W., Largier, J.L., Lessard, E.J., RaLonde, R.,
705 Rensel, J.E.J., Strutton, P.G., Trainer, V.L., Tweddle, J.F. 2012, Harmful algal blooms along
706 the North American west coast region: history, trends, causes, and impacts. Harmful Algae 19,
707 133-159.

708 Lund, J.W., Kipling, G.C., Cren, E.D. 1958. The inverted microscope method of estimating cell
709 numbers, and the statistical basis of estimation by counting. Hydrobiologia 11, 143–170.

710 Lundholm, N., Ø. Moestrup, Ø., H, AND K. Hoef-Emden, K. 2003. A study of the *Pseudo-*
711 *nitzschia pseudodelicatissima*/*cuspidata* complex (Bacillariophyceae): What is *P.*
712 *pseudodelicatissima*? J. Phycol. 39, 797–813.

713 Maldonado, M.T., M.P. Hughes, E.L. Rue, M.L. Wells. 2002. The effect of Fe and Cu
714 on growth and domoic acid production by *Pseudo-nitzschia multiseries* and *Pseudo-*
715 *nitzschia australis.* Limnol. Oceanogr. 47, 515-526.

716 MacFadyen, A., Hickey, B.M., Forman, M.G.G. 2005. Transport of surface waters from
717 the Juan de Fuca eddy region to the Washington coast. Cont. Shelf Res. 25, 2008–2021.

718 Macfadyen, A. Hickey, B.M., Cochlan, W.P. 2008. Influences of the Juan de Fuca Eddy
719 on circulation, nutrients, and phytoplankton production in the northern California
720 Current System. J. Geophys. Res. (Oceans). 113: 10.1029/2007JC004412.

721 Netto, I., Bostan, M., McCarthy, L, Laursen, A., Gilbride, K., Mehrvar, M., Pushchak, R.
722 2012. Automated image analysis of *Euglena gracilis* (Euglenophyta) for measuring
723 sublethal effects of three model contaminants. Water Sci. Technol. 66, 1708-1715.

724 Nouet, C., Motte, P., Hanikenne, M. 2011. Chloroplastic and mitochondrial metal homeostasis.
725 Trends Plant Sci. 16, 395-404.

726 O'Reilly, J.E., et.al. 2000. Ocean color chlorophyll a algorithms for SeaWiFS, OC2, and OC4:
727 Version 4. SeaWiFS Postlaunch Calibration and Validation Analyses. 11(McClain C.R., Ed.),
728 9-23., Greenbelt, Md.: Goddard Space Flight Center

729 Parsons, T. R., Maita, Y., Lalli, C.M. 1984. A Manual of Chemical and Biological Methods for
730 Seawater Analysis. xiv + 173 pp. Pergamon Press, Oxford:

731 Platt, T., Gallegos, C. L. (1980). Modelling primary production. In: P. G. Falkowski (ed.),
732 Primary Productivity in the Sea. Plenum Press, New York, p. 339-362.

733 Price, N.M., Harrison, G.I., Herring, J.G., Hudson, R.J., Nirel, P.M.V., Palenik, B., Morel,
734 F.M.M. (1988/89) Preparation and chemistry of the artificial algal culture medium Aquil. Biol.
735 Oceanogr., 6, 443-461.

736 Roy, E. 2009. The Detection and Biogeochemistry of Trace Metals in Natural Waters.
737 Ph.D. Thesis, University of Maine, Orono, Maine.

738 Rue E. L., Bruland K.W. 1995. Complexation of iron(III) by natural organic ligands as
739 determined by a new competitive equilibration/adsorptive cathodic stripping
740 voltammetry method. Mar. Chem. 50, 117–139.

741 Rue, E. and K. Bruland. 2001. Domoic acid binds iron and copper: a possible role for
742 the toxin produced by the marine diatom *Pseudo-nitzschia. Mar. Chem.* 76, 127-134.

743 Shaked, Y., and H. Lis. 2012. Disassembling iron availability to
744 phytoplankton. *Frontiers in Microbiology* 3, 123.

745 Smith, P., Bogren, K., 2001a. Determination of nitrate and/or nitrite in brackish or
746 seawater by flow injection analysis colorimeter: QuickChem Method 31-10

747 Trainer, V.L., Hickey B. M., and Horner, R.A. 2002. Biological and physical dynamics
748 of domoic acid production off the Washington U.S.A. coast. Limnol. Oceanogr. 47,
749 1438-1446.

750 Trainer, V.L, Wells, M.L., Cochlan, W.P., Trick, C.G., Bill, B.D., Baugh, K.A., Beall,
751 B.F., Herndon, J., Lundholm, N. 2009a. An ecological study of a massive toxigenic
752 bloom of *Pseudo-nitzschia cuspidata* off the Washington State coast. Limnol.
753 Oceanogr. 54, 1461-1474.

754 Trainer, V.L., Hickey, B.M., Lessard, E.J., Cochlan, W.P., Trick, C.G., Wells, M.L.,
755 MacFadyen, A., Moore. S.K. 2009b. Variability of *Pseudo-nitzschia* and domoic acid in
756 the Juan de Fuca eddy region and its adjacent shelves. Limnol. Oceanogr. 54, 289-308.

757 Trick, C.G., Wells, M.L., Cochlan, W.P., Pickell, L., McClintock, L., Ladizinsky, N.C.
758 2004. Iron limitation and copper effects in the Juan de Fuca Eddy. Ocean Sciences / The
759 Oceanic Society Meeting. Honolulu, HI.

760 Radan, R.L., Cochlan, W.P. 2018. Differential toxin response of *Pseudo-nitzschia*
761 *multiseries* as a function of nitrogen speciation in batch and continuous cultures, and
762 during a natural assemblage experiment. Harmful Algae 73, 12-29.

763 Smith, P., Bogren, K., 2001. Determination of nitrate and/or nitrite in brackish or
764 seawater by flow injection analysis colorimetry: QuikChem® Method 31-107-04-1-E.
765 Lachat Instruments, Milwaukee, WI, 12 pp.

766 Wells, M.L. 1999. Manipulating iron availability in nearshore waters. Limnol. Oceanogr.
767 44, 1002-1008.

768 Wells, M.L., Trick, C.G. 2004. Controlling iron availability to phytoplankton in iron-
769 replete coastal waters. Mar. Chem. 86, 1–13.

770 Wells, M.L., Trick, C.G., Cochlan, W.P., Beall, B., 2009. Persistence of iron limitation in
771 the western subarctic Pacific SEEDS II mesoscale fertilization experiment. Deep Sea Res.
772 Part II 56, 2810-2821.

773 Wells, M.L., Trick, C.G., Cochlan, W.P., Hughes, P., Trainer, V.T. 2005. Domoic acid:
774 The synergy of iron, copper, and the toxicity of diatoms. Limnol. Oceanogr. 50, 1908–
775 1917

776 Welschmeyer, N.A. 1994. Fluorometric analysis of chlorophyll *a* in the presence of
777 chlorophyll *b* and pheopigments. Limnol. Oceanogr. 39, 1985-1992.

778 Wolters, M., 2002. Determination of silicate in brackish or seawater by flow injection
779 analysis. QuikChem® Method 31-114-27-1-D. Lachat Instruments, Milwaukee, WI, 12
780 pp.

781